

This article was downloaded by:

On: 17 January 2011

Access details: *Access Details: Free Access*

Publisher *Taylor & Francis*

Informa Ltd Registered in England and Wales Registered Number: 1072954 Registered office: Mortimer House, 37-41 Mortimer Street, London W1T 3JH, UK



International Journal of Environmental Analytical Chemistry

Publication details, including instructions for authors and subscription information:

<http://www.informaworld.com/smpp/title~content=t713640455>

Calibration of a Multipoint Sampling System Connected with a Photoacoustic Detector

Alex de Visscher^a; Annick Goossens^a; Oswald van Cleemput^a

^a Laboratory of Applied Physical Chemistry, Faculty of Agricultural and Applied Biological Sciences, University of Ghent, Gent, Belgium

To cite this Article de Visscher, Alex , Goossens, Annick and van Cleemput, Oswald(2000) 'Calibration of a Multipoint Sampling System Connected with a Photoacoustic Detector', *International Journal of Environmental Analytical Chemistry*, 76: 2, 115 — 133

To link to this Article: DOI: 10.1080/03067310008034124

URL: <http://dx.doi.org/10.1080/03067310008034124>

PLEASE SCROLL DOWN FOR ARTICLE

Full terms and conditions of use: <http://www.informaworld.com/terms-and-conditions-of-access.pdf>

This article may be used for research, teaching and private study purposes. Any substantial or systematic reproduction, re-distribution, re-selling, loan or sub-licensing, systematic supply or distribution in any form to anyone is expressly forbidden.

The publisher does not give any warranty express or implied or make any representation that the contents will be complete or accurate or up to date. The accuracy of any instructions, formulae and drug doses should be independently verified with primary sources. The publisher shall not be liable for any loss, actions, claims, proceedings, demand or costs or damages whatsoever or howsoever caused arising directly or indirectly in connection with or arising out of the use of this material.

CALIBRATION OF A MULTIPOINT SAMPLING SYSTEM CONNECTED WITH A PHOTOACOUSTIC DETECTOR

ALEX DE VISSCHER*, ANNICK GOOSSENS and
OSWALD VAN CLEEMPUT

*Laboratory of Applied Physical Chemistry, Faculty of Agricultural and Applied
Biological Sciences, University of Ghent, Coupure Links 653, B-9000 Gent, Belgium*

(Received 23 March 1999; In final form 17 June 1999)

Photoacoustic detection of gases in the air phase in combination with a multipoint sampling device transfers about 100 mL of air from each sample location to the next one, causing a considerable disturbance when small systems are sampled. In reactive systems, such as trace gas exchange in soil samples, a correction is required to determine the kinetic behavior of the systems. But this kinetic behavior is required in turn to calculate the correction in a repeated sampling sequence. A model was developed for reaction kinetics (zero-order or first-order) within closed systems and the sample transfer between these systems by a CBISS MK2 multipoint sampling system, connected with a Brüel & Kjær photoacoustic detector. By regression, the reaction kinetics is determined, and by simulation of the system in the absence of sample transfer, corrected data are generated. Comparison of experimental and modeled data revealed that part of the sample is transferred directly two systems further. In addition, a slight memory effect of the detector was revealed. These effects were accounted for in the model. If the correction is not made, biased results are obtained for the reaction kinetics.

Keywords: Photoacoustic detector; trace gases; gas sampling; calibration

INTRODUCTION

Photoacoustic detection is a convenient method for analysis of trace gases such as methane (CH_4) and nitrous oxide (N_2O) in the atmosphere^[1,2]. In combination with a multipoint gas sampler, it provides a valuable tool for studying trace gas biogeochemical reactions in the field and in microcosm experiments, where high variabilities occur. However, such multipoint sampling system transfers a considerable air volume from each ecosystem or microcosm to the next one, on the

* Corresponding author. Fax: +32-9-2646242. E-mail: alex.devisscher@rug.ac.be

order of 100 mL. So, when systems with an air volume of only a few liters are sampled repeatedly, the disturbances accumulate, and have to be accounted for. Velthof and Oenema^[1] used this system in a field study of N₂O emissions from grassland. Fluxes were determined by measuring the N₂O accumulation in six bottomless boxes that were pressed into the soil. The transfer of N₂O between the boxes was accounted for with a careful bookkeeping of the amounts of N₂O transferred. Each amount was compensated for mathematically, thus obtaining concentrations of hypothetically undisturbed boxes. This method is justified in the case of Velthof and Oenema because the fluxes were approximately zero-order, so the N₂O concentration in the boxes did not affect the fluxes. However, whenever the reaction kinetics of a system deviates from zero-order, the transfer of trace gas, which alters the concentration in the system, will influence the reaction rate. Consequently, knowledge on the reaction kinetics of the system is required in order to calculate these corrections that have to be made, and the corrections are required in order to determine the reaction kinetics, so the method of Velthof and Oenema cannot be used in such a case. N₂O emissions that deviate from zero-order kinetics have been observed experimentally^[3,4]. The oxidation of atmospheric CH₄ by soil microorganisms is first-order^[5]. Clearly, there is a need for a method to account for sample transfer between closed systems with reaction kinetics deviating from zero-order.

Aim of this study is to develop such a method. Basically, the method involves a simulation of the kinetic behavior of the systems and the sample transfer between the systems. This simulation model is then fitted to the experimental data by non-linear regression. Then, a simulation of the kinetic behavior of the systems in the absence of sample transfer yields the corrected data.

EXPERIMENTAL

Experimental setup

The experiments were performed with a CBISS MK2 multipoint sampling system, connected with a Brüel & Kjær photoacoustic detector. All connections were made with Teflon tubes. The multisampler was connected to six glass jars (volume 1.212 L including the connection tubes). Figure 1 shows a detailed representation of the equipment and the experimental setup. The total internal volume of the sampler and the analyzer was given by the manufacturer. This volume depends on the sample port, and is given in Table I. During sampling, air was taken from the appropriate jar at maximum 30 mL s⁻¹ to rinse the tubing, the

sampler and the analyzer in a first step. Rinsing time depended on the tubing length. In a second step, the cell was rinsed during 11 s at maximum 5 mL s^{-1} .

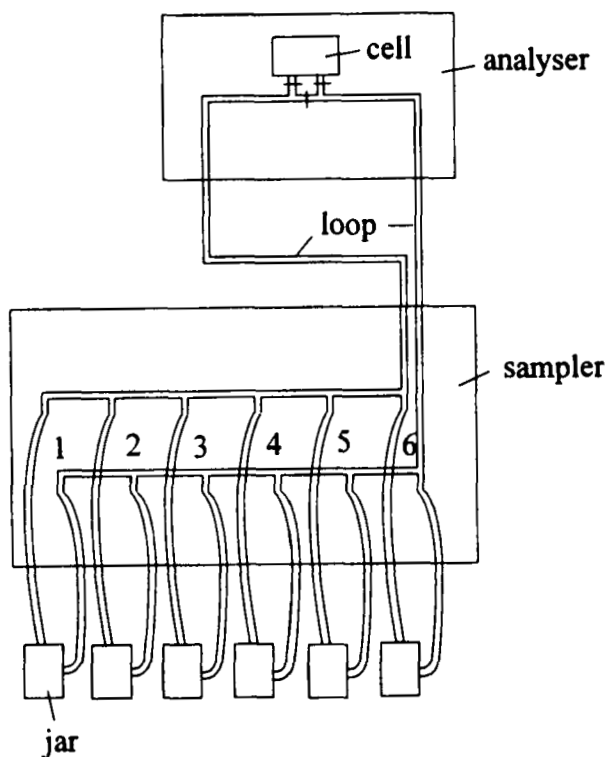


FIGURE 1 Setup of the photoacoustic detector and the multipoint sampler, connected to 6 microcosms

TABLE I Internal volume of the Brüel & Kjær analyzer and the CBISS sampler

Sample port	Volume (mL)
1	66.72
2	64.22
3	61.72
4	59.22
5	56.72
6	54.22

Two experiments were performed. The first experiment was in the absence of reactions and was performed to determine the characteristics of the sample transfer process, that is, to calibrate the sample transfer part of the simulation model. For this experiment, 3 jars were filled with an equal volume of CH_4 up to about $68 \mu\text{L/L}$, and connected to sample ports 1–3. The other 3 jars were filled with laboratory air, which contained about $4 \mu\text{L/L}$ CH_4 , and were connected to sample ports 4–6. The second experiment was performed in the presence of soil, in order to determine the reaction kinetics of CH_4 oxidation in the soil. About 50 g of soil was added to jar 1–5. This soil had been exposed to high CH_4 mixing ratios in a setup described earlier^[6], and had a high capacity for CH_4 oxidation. Jar 6 was kept empty. Jar 1–5 was filled up to about $65 \mu\text{L/L}$ CH_4 . No CH_4 was added to jar 6.

Data analysis

In order to analyze the data, a program was developed that can be subdivided roughly into 3 sections: a sample transfer simulation section, a reaction kinetics section, and a fitting section. The sample transfer simulation section has several options. We will discuss the simplest version of the sample transfer model in this section of the paper. The more detailed versions will be discussed in the Results and Discussion section, when they apply. The reactions occur in 6 jars with head-space volumes V_{jar} . This volume includes the sample tubes between the jars and the multipoint sampler. The volume of the sample tubes between the sampler and the analyzer is V_{loop} , the internal volume of the sampler and the analyzer is V_i when jar i ($i = 1, \dots, 6$) is analyzed. The values of V_i are given in Table I. The following variables are defined:

C_{jar}^{i-} the concentration of the analyzed compound in jar i just before sampling

C_{jar}^{i+} the concentration of the analyzed compound in jar i just after sampling

C_{loop}^- the concentration of the analyzed compound in the loop just before sampling

C_{loop}^+ the concentration of the analyzed compound in the loop just after sampling

C_{trap}^i the concentration of the analyzed compound trapped after sampling jar i

Initially, C_{loop}^- and C_{trap}^i have ambient values. The value of C_{jar}^{i+} can be calculated with a mass balance, given the value of C_{jar}^{i-} . We assume that the entire volumes V_{loop} and V_i are rinsed completely in the sampling process. So, cell and loops contain air with the same composition as the air in the sampled jar. After

sampling each of the jars 1–5, an air volume of 2.5 mL is trapped due to the sample volume differences. All these trapped volumes are released during the sampling process of jar 1, and mixed with the air in the box.

After sampling, C_{loop}^+ and C_{trap}^i have new values, equal to C_{jar}^{i+} . C_{loop}^+ is the concentration that is observed by the detector. This mode of calculation is referred to as the base model.

When a cycle of 6 samplings is completed, the reaction kinetics section comes into play. When the program is used for determining the value of V_{loop} (data analysis of experiment 1, calibration), there are no reactions, and the concentrations in the boxes just before the second sampling, C_{jar}^{i-} , equals the concentrations after the first sampling, C_{jar}^{i+} .

When the program is used for analyzing kinetic data (experiment 2), the equations depend on the type of kinetics. For instance, if zero-order kinetics of the analyzed compound is applied, a kinetic constant $k_{0,i}$ is defined for each box i . The concentrations in the boxes just before the second sampling is calculated as follows:

$$C_{jar}^{i-} = C_{jar}^{i+} + k_{0,i}\Delta t \quad (1)$$

with Δt the time between subsequent samplings of the same jar. In the case of first-order degradation kinetics, a kinetic constant $k_{1,i}$ is defined for each jar i . The equation is as follows:

$$C_{jar}^{i-} = C_{jar}^{i+} \exp(-k_{1,i}\Delta t) \quad (2)$$

In principle any kinetic equation can be used. In all cases the compound to be analyzed is assumed to be stable in the loop, so $C_{loop}^- = C_{loop}^+$.

The fitting section of the program drives the other two sections. When the program is used for determining V_{loop} (experiment 1, calibration), the program simulates the measured concentrations with initial guesses of V_{loop} and the initial concentrations supplied by the user. These simulated concentrations are compared with the measured concentrations. The values of V_{loop} and the initial concentrations in the jars are adapted iteratively by nonlinear regression until the simulated concentrations are optimized, i.e., until the sum of the squares of the deviations between measured and calculated concentrations is minimized. A Levenberg-Marquardt routine is used for regression^[7].

When the program is used to analyze kinetic data, the value of V_{loop} is kept constant at the (calibrated) value supplied by the user, and the values of $k_{0,i}$ (zero-order) or $k_{1,i}$ (first-order) are optimized, together with the initial concentrations.

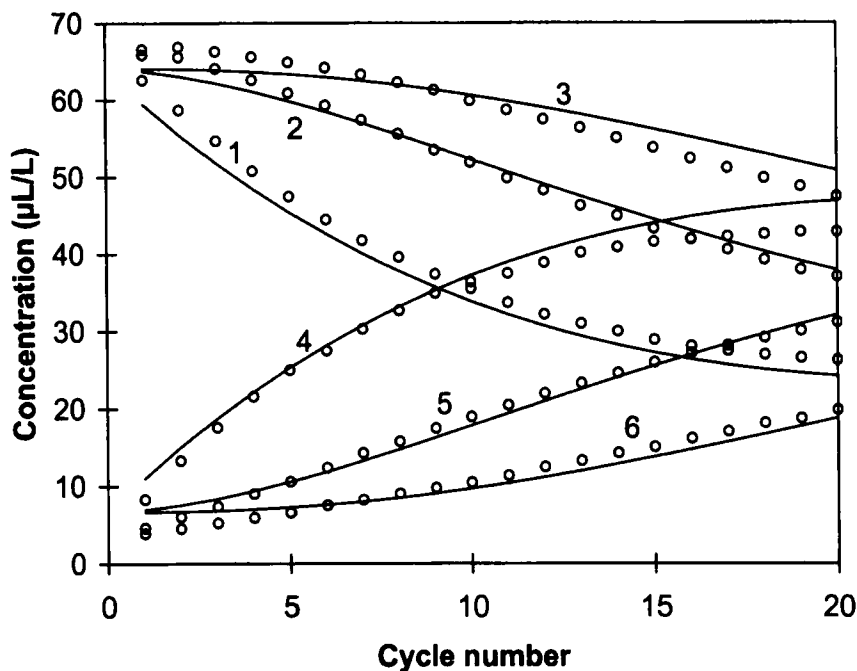


FIGURE 2 Experimentally observed evolution of the CH_4 concentrations (circles) in jars 1–6 (numbers on graphs) due to sample transfer, with the results of the fitted base model (curves)

RESULTS AND DISCUSSION

Calibration

Figure 2 shows the results of the first experiment, in the absence of chemical reactions, with the simulated results obtained in the calibration for V_{loop} with the base model. The estimated loop volume was 40.8 ± 2.5 mL (all error data have 95% uncertainty margins). This slightly exceeded the expected value of 31 mL. The initial concentrations in jars 1–3 were assumed to be the same. This was also assumed for jars 4–6. The estimated initial concentrations were 64.12 ± 0.64 $\mu\text{L/L}$ in jars 1–3, and 6.61 ± 0.63 $\mu\text{L/L}$ in jars 4–6. The standard deviation between the experimental data and the calculated data was 1.7 $\mu\text{L/L}$. It is clear from Figure 2 that there was a considerable amount of mixing between the jars. Jar 1 lost more than half of its CH_4 concentration. Jar 4 gained about 35 $\mu\text{L/L}$ of CH_4 . The air in jars 2 and 5 underwent a concentration change of over 25 $\mu\text{L/L}$. In the case of

jars 3 and 6, the concentration change was less than 20 $\mu\text{L/L}$. The concentration change depended on the concentration in the preceding jar. Jar 1 received CH_4 from jar 6, which contained almost no CH_4 in the first half of the experiment. As a result, the CH_4 concentration in jar 1 decreases sharply in that period. Jar 2 receives CH_4 from jar 1, so the concentration decrease in jar 2 becomes pronounced only when the concentration in jar 1 has decreased sufficiently. The same reasoning can be applied to the other jars. Comparison between the experimental and the modeled results reveals that the model underestimates the concentration changes in jars 2, 3, 5, and 6. The overall fit between the model and the experiments is not very good. This suggests that each jar also receives CH_4 from two jars before. This is what happens when the sampler and the analyzer are rinsed incompletely. A sample transfer model was developed that accounted for incomplete rinsing of sampler, analyzer, and the tubing between them. It was assumed that the concentration was the same in sampler, analyzer, and tubing in between, but different from the concentration in the jar. This model did not improve the fit between theory and experiment (data not shown). So, the mechanism for sample transfer between non-neighbouring jars must have been different. Close examination of the sampling process reveals the mechanism. In a first step, the sampler and the tubing are rinsed completely, but the cell is not. The cell is rinsed with a much smaller air volume in a second step. So, after the sampling process, the air from the cell is now inside the sampler and the tubing between the analyzer and the sampler. In the first step of the sampling process after that, this air volume is rinsed out, into the second jar after the one from which the air originates. A sample transfer model was developed for the simulation of this process. First, some new variables are defined:

V_{cell} the volume of the cell (mL)

C_{cell}^- the concentration of the analyzed compound in the cell before sampling ($\mu\text{L/L}$)

C_{cell}^+ the concentration of the analyzed compound in the cell after sampling ($\mu\text{L/L}$)

The procedure of the base model can be used to describe the first step in the sampling process in the present case. C_{jar}^{i+} is the concentration in the jar after step 1. Since it is assumed that the contents of the cell are transferred to the loop in the second step, it is assumed that C_{jar}^{i+} stays the same in this step, as well as C_{trap}^i , the concentration trapped. C_{loop}^+ is the concentration in the loop after step 1 of the sampling process. The calculation of the concentration in the loop and in the cell after step 2 of the sampling process is based on the schematic representation on Figure 3. From this scheme, it is clear that C_{cell}^+ after step 2 equals the value of C_{loop}^+ after step 1. Furthermore:

$$C_{loop}^{++} = \frac{(V_{loop} + V_i - V_{cell})C_{loop}^{+} + V_{cell}C_{cell}^{-}}{V_{loop} + V_i} \quad (3)$$

C_{loop}^{++} is the average concentration in the loop after step 2 of the sampling process.

C_{cell}^{+} is the concentration observed experimentally. This mode of calculation is referred to as the two-step model.

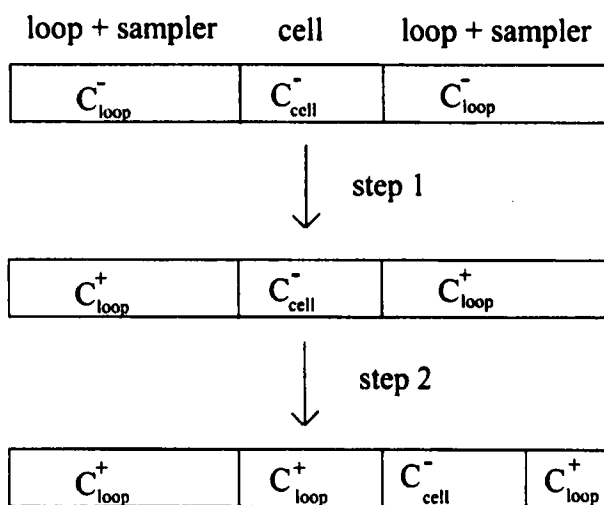


FIGURE 3 Schematic representation of the air composition in the detector cell and the sample loop during the sampling process according to the two-step model

Figure 4 shows the result of the calibration with the two-step model. The fit between theory and experiment has clearly been improved (standard deviation $0.75 \mu\text{L/L}$). Only a slight systematic deviation is apparent in the concentration development of the jars. The loop volume is estimated at $38.5 \pm 1.2 \text{ mL}$, the cell volume at $17.5 \pm 1.5 \text{ mL}$, the initial concentrations $66.79 \pm 0.37 \mu\text{L/L}$ in jars 1–3, and $4.08 \pm 0.36 \mu\text{L/L}$ in jars 4–6.

There is a possibility that part of the cell air returns to the jar in the second step of the sampling process instead of in the loop. Mathematically, this situation cannot be distinguished from the one modeled here with a smaller cell volume and a larger loop volume. Therefore, no effort is made to account for this effect. Note, however, that the loop volume estimate is indeed larger than the measured value (31 mL). So, it must be stressed that the calibration must be repeated whenever

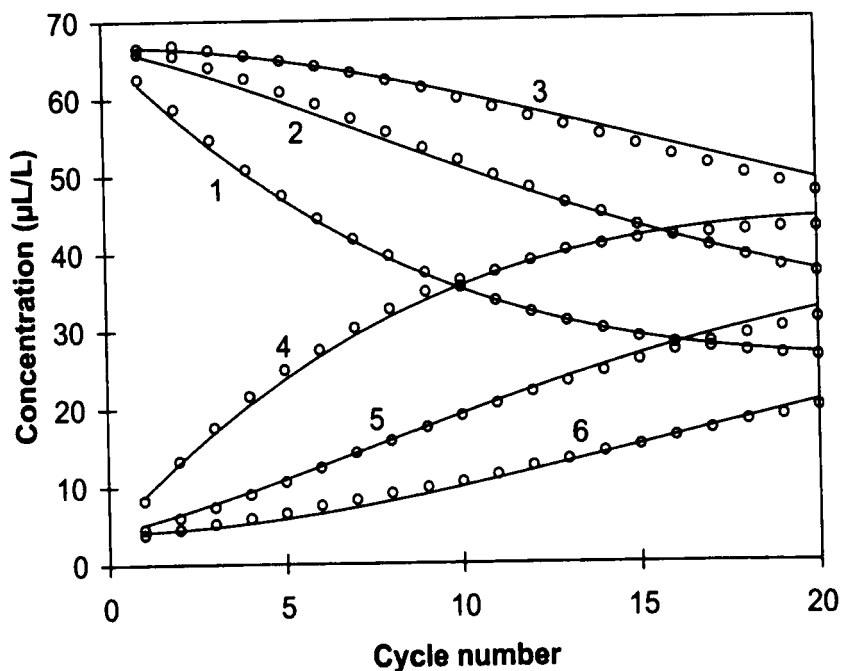


FIGURE 4 Experimentally observed evolution of the CH_4 concentrations (circles) in jars 1–6 (numbers on graphs) due to sample transfer, with the results of the fitted two-step model (curves)

the sample loop is replaced, unless the volume of the new sample loop is exactly the same as the volume of the old one.

It is also possible that the cell is not rinsed completely, as rinsing a 17.5 mL volume with maximum 55 mL of air is not necessarily 100% effective, depending on cell geometry. This was checked with a slightly modified setup. Jar 1 (2130 mL, including tubing between the jar and the sampler) was filled with CH_4 (84 $\mu\text{L/L}$). The inlets of sample points 2–4 drew air from the open air outside the laboratory. The outlets of sample ports 2–4 were not connected to any tubing, so the air drawn from outside was released in the laboratory. This setup completely excludes backmixing of cell air into the sampler, so any 'memory effect' occurring during the analysis of sample ports 2–4 must be due to incomplete rinsing. Sample ports 5–6 were not used during this experiment. An average memory effect of 0.9165% was apparent from this experiment. So, this effect has to be accounted for in the analysis. The concentration difference between jar 1 and the ambient CH_4 concentration decreased exponentially with cycle number, with a concentration decrease of $5.75 \pm 0.14\%$ per cycle. So, each cycle a volume of

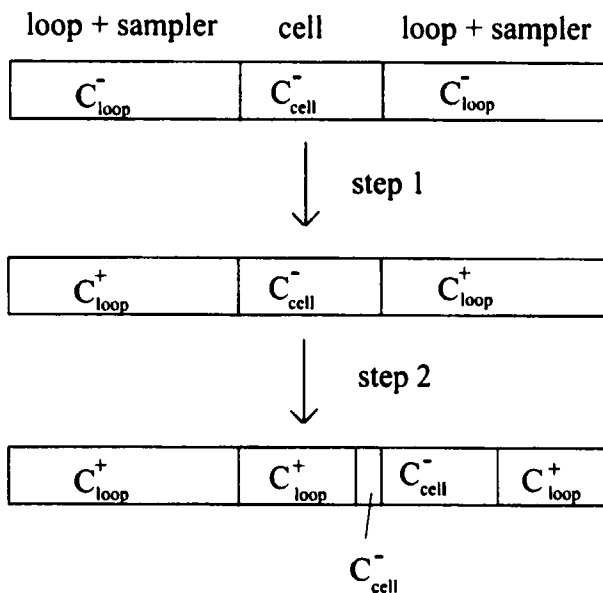


FIGURE 5 Schematic representation of the air composition in the detector cell and the sample loop during the sampling process according to the two-step model with incomplete cell mixing

$(0.0575 \pm 0.0014) \times 2130 \text{ mL} = 122.4 \pm 2.9 \text{ mL}$ was replaced in this jar. This volume should equal $V_2 + V_{\text{loop}} + V_{\text{cell}}$ in the case of the previous model. Filling in the estimated parameter values yields an estimated volume of 120.2 mL, not significantly different from the volume obtained here. This shows that the model can be extrapolated to a different setup, with a different jar volume.

A model was developed for the sample transfer in the case of incomplete rinsing of the cell. The process is visualised schematically in Figure 5. We define V_{over} as the cell volume that is not rinsed. Step 1 of the sampling process is identical to step 1 in the previous model. The average concentration of the analyzed compound in the cell after step 2 is given by the following equation:

$$C_{\text{cell}}^+ = \frac{(V_{\text{cell}} - V_{\text{over}})C_{\text{loop}}^+ + V_{\text{over}}C_{\text{cell}}^-}{V_{\text{cell}}} \quad (4)$$

The average concentration in the loop is:

$$C_{\text{loop}}^{++} = \frac{(V_{\text{loop}} + V_i - (V_{\text{cell}} - V_{\text{over}}))C_{\text{loop}}^+ + (V_{\text{cell}} - V_{\text{over}})C_{\text{cell}}^-}{V_{\text{loop}} + V_i} \quad (5)$$

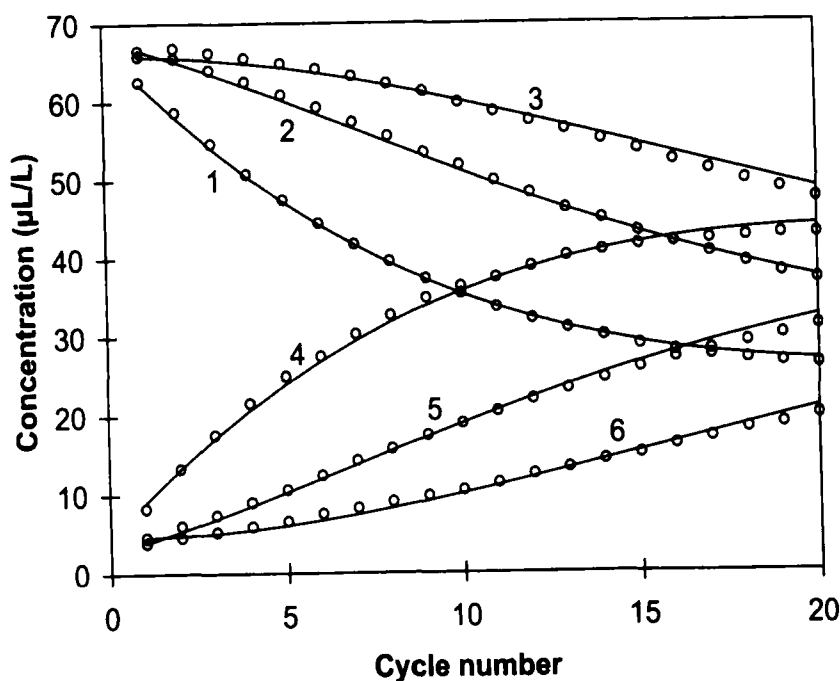


FIGURE 6 Experimentally observed evolution of the CH_4 concentrations (circles) in jars 1–6 (numbers on graphs) due to sample transfer, with the results of the fitted two-step model with incomplete mixing (curves) (all initial concentrations optimized)

These equations allow simulation of the sample transfer with incomplete mixing of the cell. They are referred to as the two-step model with incomplete cell mixing. Based on these calculations, a new regression was performed. First, this regression was performed with a fixed value of V_{over} of 0.009165×17.5 mL. It provided a new estimate of V_{cell} . The regression was repeated with a V_{over} value of 0.009165 times the new estimate of V_{cell} . This procedure was repeated until convergence of the parameter estimates. The new parameter values were 37.6 ± 1.2 mL for V_{loop} , 18.3 ± 1.5 mL for V_{cell} , and 0.168 mL for V_{over} . The initial concentration in jars 1–3 was estimated at 66.98 ± 0.37 $\mu\text{L/L}$; in jars 4–6 it was estimated at 3.90 ± 0.36 $\mu\text{L/L}$. The standard deviation of the model was estimated at 0.76 $\mu\text{L/L}$, practically the same as with complete rinsing of the cell. In this case $V_2 + V_{\text{loop}} + V_{\text{cell}}$ equals 120.1 mL, again not significantly different from the determination with the different setup. The simulated evolution of the concentrations was not markedly different from the evolutions in Figure 4. Therefore, the data are not shown.

Slight differences between the initial concentrations in jars 1–3 and jars 4–6 may have occurred. Therefore, the calibration was repeated, and the initial concentrations in all jars were allowed to evolve separately to an optimum value. The result is shown in Figure 6. The standard deviation of the model is estimated at 0.66 $\mu\text{L/L}$. This is slightly less than the previous two cases, but the difference is not significant. The estimated initial concentrations were the following in jars 1–6: 67.97 ± 0.77 $\mu\text{L/L}$, 67.92 ± 0.76 $\mu\text{L/L}$, 65.78 ± 0.60 $\mu\text{L/L}$, 3.79 ± 0.75 $\mu\text{L/L}$, 2.60 ± 0.73 $\mu\text{L/L}$, and 4.55 ± 0.58 $\mu\text{L/L}$. V_{loop} was 39.5 ± 1.7 mL, V_{cell} was 19.4 ± 1.7 mL, and V_{over} was 0.178 mL. In this case $V_2 + V_{\text{loop}} + V_{\text{cell}}$ equals 123.1 mL, very close to the measurement with the larger jar (122.4 ± 2.9 mL). We used these parameters in the two-step model with incomplete cell mixing in the next section.

Kinetic analysis

Figure 7 shows the results of the experiment with the CH_4 oxidizing soil. The time between two sample analyzes was 3 minutes. Consequently, the time between subsequent sample cycles was 18 minutes. Again considerable mixing was apparent in the empty jar. The other concentration curves did not seem to deviate substantially from first-order degradation kinetics, which might suggest that the distortions due to sample transfer were not very important. Figure 8 shows the model results together with the calculated undisturbed CH_4 concentrations. It is clear that sample transfer did influence the evolution of the concentration. A comparison of the kinetic constants with and without accounting for the sample transfer leads to the same conclusion. Table II shows the kinetic constants obtained with our model, and the kinetic constants obtained by fitting first-order kinetics to the uncorrected data of Figure 7. Clearly there is a significant influence of sample transfer, and the correction developed is required to assess the kinetic behavior of trace gas exchange between the atmosphere and soils correctly.

TABLE II Degradation rates k_1 (min^{-1}) of CH_4 in the jars with and without correction for sample transfer

Jar	k_1 with correction (min^{-1})	k_1 without correction (min^{-1})
1	$8.93 \times 10^{-4} \pm 1.82 \times 10^{-4}$	$3.05 \times 10^{-3} \pm 1.03 \times 10^{-4}$
2	$5.86 \times 10^{-3} \pm 3.31 \times 10^{-4}$	$4.43 \times 10^{-3} \pm 2.54 \times 10^{-4}$
3	$9.69 \times 10^{-3} \pm 5.12 \times 10^{-4}$	$6.09 \times 10^{-3} \pm 4.90 \times 10^{-4}$
4	$1.02 \times 10^{-2} \pm 6.21 \times 10^{-4}$	$7.35 \times 10^{-3} \pm 5.56 \times 10^{-4}$
5	$8.55 \times 10^{-3} \pm 4.93 \times 10^{-4}$	$7.62 \times 10^{-3} \pm 3.48 \times 10^{-4}$
6	$-8.77 \times 10^{-5} \pm 3.75 \times 10^{-4}$	$3.61 \times 10^{-4} \pm 7.68 \times 10^{-4}$

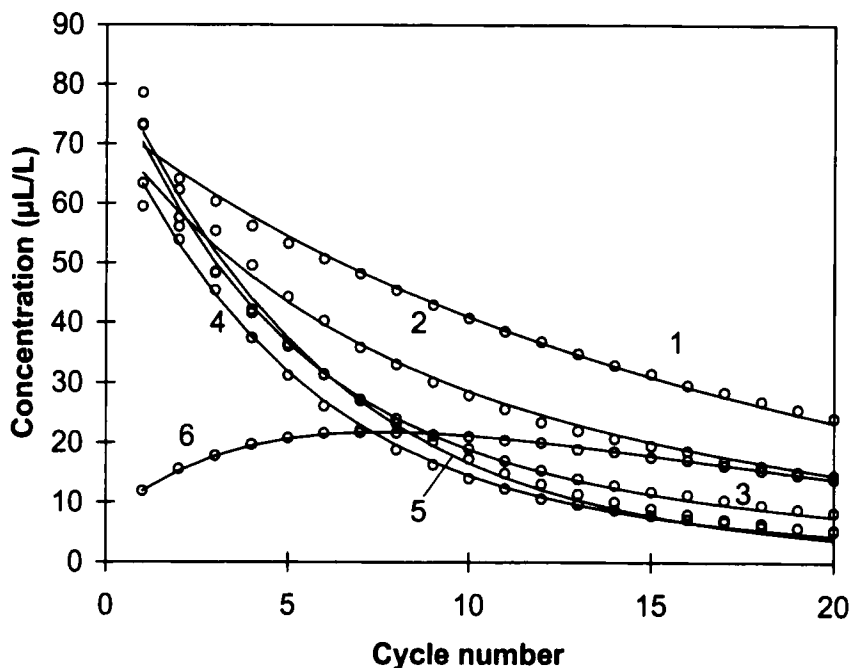


FIGURE 7 Experimental (circles) and fitted (curves) CH_4 concentrations of the CH_4 oxidation experiment

The sample mixing effect is less important as the jar headspace volumes increase. We will now calculate the minimum headspace volume required for the mixing effect to be negligible. First, we consider the case of a field experiment, where coefficients of variance of gas fluxes are typically on the order of 50–200%^[8]. Table III shows two series of 6 numbers, both with average value 1. The series have standard deviations of 0.5 (CV = 50%) and 2 (CV = 200%), respectively. Distributions of reaction rates around a given average value can be obtained by multiplying the values in Table III by the average reaction rate. The analysis was restricted to first-order degradation kinetics. With a given set of reaction rates and a given jar volume, the expected evolution of the concentration of the reactive compound in the jars due to reaction and sample transfer is calculated, and apparent reaction rate constants were calculated from these data with linear regression based on the logarithm of the concentrations. These apparent reaction rates were compared with the real values.

The influence of sample transfer depends on the reaction rate multiplied by the time between subsequent samples of the same jar, rather than the reaction rates

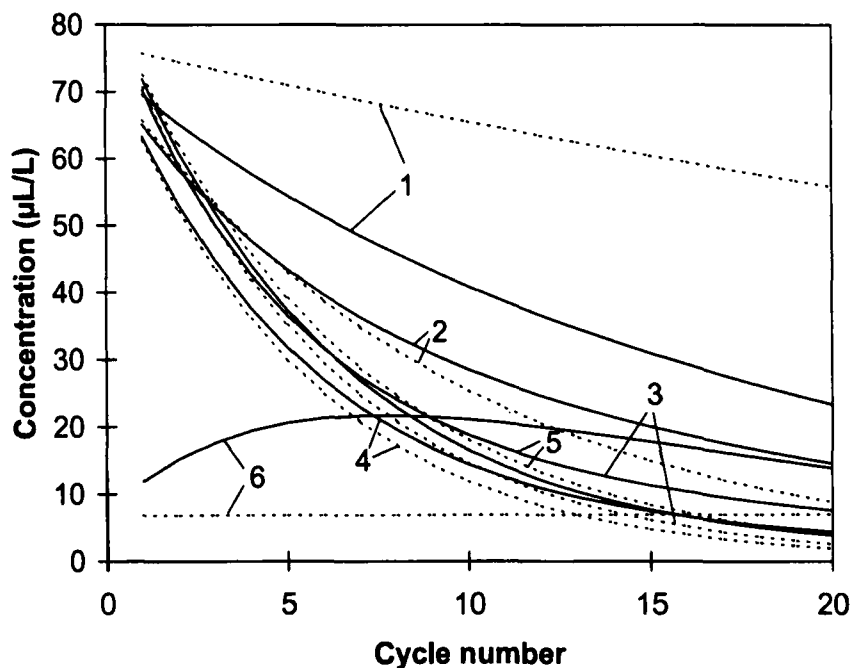


FIGURE 8 Uncorrected (solid curves) and corrected (dotted curves) CH_4 concentration evolution of the CH_4 oxidation experiment (model results)

itself. Also, the influence depends on the reduced jar volume (jar volume divided by the transferred sample volume, $V_1 + V_{\text{loop}} + V_{\text{cell}}$), rather than the absolute jar volume. Therefore, calculations were performed with $k_{\text{av}} t$ values (k_{av} = average reaction rate constant, t = time between subsequent samples of the same jar) ranging from 0.1 to 0.7. $k_{\text{av}} t = 0.1$ corresponds approximately with a 10% concentration decrease per sample; $k_{\text{av}} t = 0.7$ corresponds with a 50% decrease per sample. The case of 5 samples per jar is compared with the case of 10 samples per jar.

Figure 9 shows the apparent $k_i t$ values (k_i = apparent reaction rate constant in jar i) as a function of the reduced volume, for $k_{\text{av}} t = 0.1$ and $\text{CV} = 50\%$. When 5 samples are taken, all k_i values are within 10% of the real values when the reduced volume exceeds 38. In the case of 10 samples per jar, the reduced volume must exceed 67. In the case of the present setup, this means jar volumes of 4.8 L and 8.4 L, respectively. When $\text{CV} = 200\%$, no accurate determinations of k_i are possible without the model. Due to the large concentration differences between the jars, the memory effect of the cell becomes important. Therefore, the analysis is restricted to the case of $\text{CV} = 50\%$.

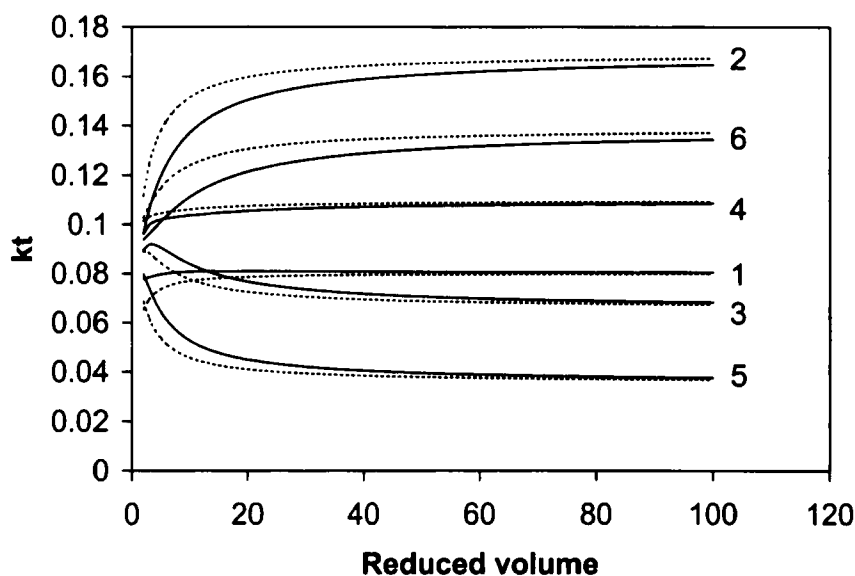


FIGURE 9 Apparent degradation rates in 6 jars versus reduced jar volume (= jar volume/mixed sample volume), due to sample mixing. Real average $kt = 0.1$; coefficient of variance = 50%. Dotted curves: 5 samples per jar; solid curves: 10 samples per jar; jar numbers are indicated in graph

TABLE III Series of numbers with average value 1 and standard deviation (SD) as indicated

Jar	Series 1 ($SD = 0.5$)	Series 2 ($SD = 2$)
1	0.7972	0.4267
2	1.7028	0.15
3	0.65	5.0733
4	1.1	0.05
5	0.35	0.22
6	1.4	0.08

Figure 10 shows the normalized average value of the reaction rate (calculated $k_{av} t / \text{exact } k_{av} t$) as a function of the reduced volume. From a statistical point of view, none of the calculated average values differs significantly from the real average values, but the calculated values are biased. When the model is not used for correction, degradation rates will be underestimated systematically. In order to limit biased results to a few percents without correction, the sampling interval should be chosen sufficiently short, so $k_{av} t < 0.4$ when 5 samples are taken per jar, and $k_{av} t < 0.1$ when 10 samples are taken. A disadvantage of this is of course the reduced accuracy if very short sampling intervals are taken.

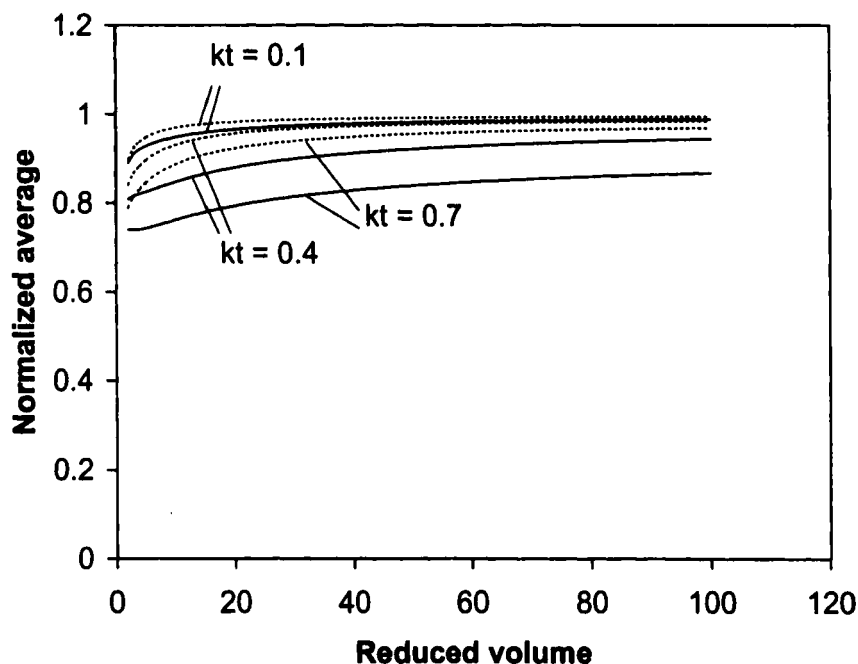


FIGURE 10 Normalized average value of kt (= apparent average/real average) versus reduced jar volume (= jar volume/mixed sample volume), due to sample mixing. Coefficient of variance = 50%. Dotted curves: 5 samples per jar; solid curves: 10 samples per jar

Figure 11 shows the estimated coefficient of variation when the real CV is 50%. Values exceeding 19% are not statistically different from 50%, which is usually the case. Again, the value is systematically underestimated due to the mixing effect, which may be important in geostatistical applications.

As a second case, a laboratory situation is considered. Three samples with a given average reaction rate are compared with three samples that are half as reactive (e.g., due to addition of an inhibitor). Both populations have a CV of 10%, which is typical for well-mixed soil samples in laboratory conditions. Again, first-order reaction kinetics are considered. The sequence used for calculating the reaction rates is 1,1,1,0.9,0.5,0.55,0.45.

Figure 12 shows the normalized average value of the reaction rate as a function of the reduced volume. The mixing effect and the detector memory effect have a much larger influence on jars 1–3 than on jars 4–6. This is because the concentrations reach lower values in jars 1–3, where the reaction rates are higher. If an environment is contaminated with air at a lower concentration of the reactive compound than the environment itself, the influence cannot be larger than the

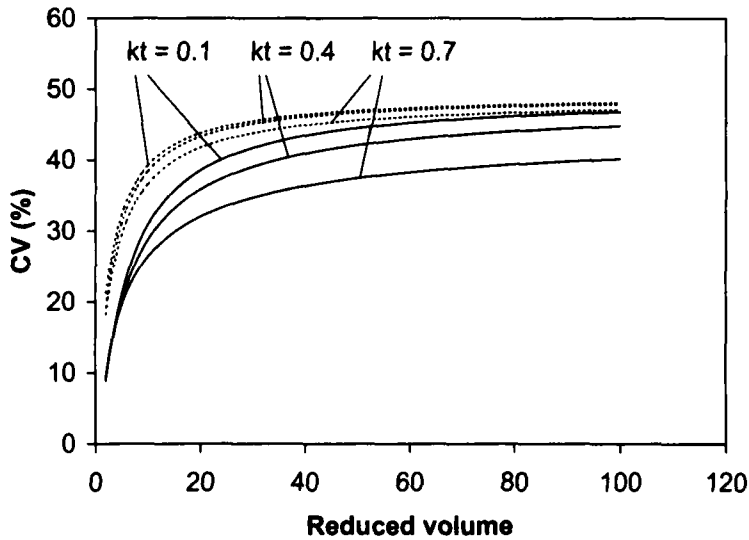


FIGURE 11 Apparent coefficient of variance versus reduced jar volume (= jar volume/mixed sample volume), due to sample mixing. Real coefficient of variance = 50%. Dotted curves: 5 samples per jar; solid curves: 10 samples per jar

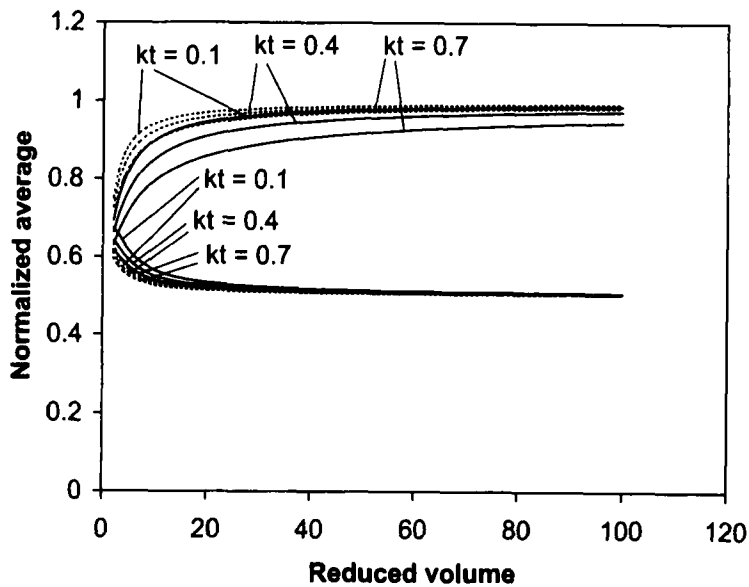


FIGURE 12 Normalized average value of kt (= apparent average/real average) versus reduced jar volume (= jar volume/mixed sample volume), due to sample mixing. Real average kt values are 1 (CV = 10%) in jars 1–3 (indicated 1–3 in graph) and 0.5 (CV = 10%) in jars 4–6 (indicated 4–6 in graph). Dotted curves: 5 samples per jar; solid curves: 10 samples per jar

dilution effect of repeatedly withdrawing air. This is what happens in jars 4–6. In jars 1–3, the contamination can be much stronger due to the relatively high concentration in jars 4–6. Again, the bias can be limited to a few percents by choosing the sampling interval sufficiently short, so $k_{av} t < 0.4$ when 5 samples are taken per jar, and $k_{av} < 0.1$ when 10 samples are taken.

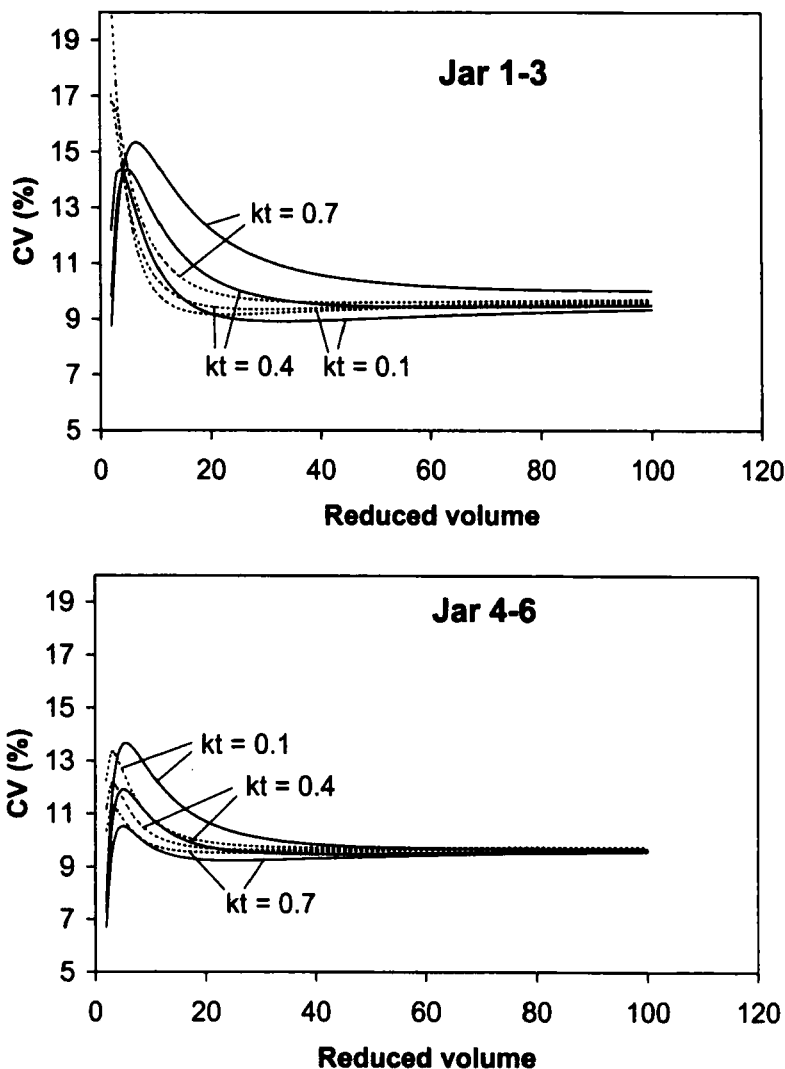


FIGURE 13 Apparent coefficients of variance in jars 1–3 and jars 4–6 versus reduced jar volume (= jar volume/mixed sample volume), due to sample mixing. Real CV is 10% in both jars 1–3 and jars 4–6. Dotted curves: 5 samples per jar; solid curves: 10 samples per jar

Figure 13 shows the estimated coefficients of variation. In this case the CV values are generally overestimated, because environments with different reaction kinetics contaminate each other. Without corrections, reduced volumes of at least 30 are preferable.

To conclude, our model is able to correct for sample transfer and memory effects of the detector. Without the model, biased results are obtained. The bias can be minimized by working with large microcosms, and by keeping the sampling interval sufficiently short. In the case of extreme variability, accurate measurements are impossible without the correction, due to the memory effect of the detector.

Acknowledgements

The Prime Minister's Office – Federal Office for Scientific, Technical, and Cultural Affairs is acknowledged for financial support.

References

- [1] G. L. Velthof and O. Oenema, *Eur. J. Soil Sci.*, **46**, 533–540 (1995).
- [2] P. Ambus and G. P. Robertson, *Soil Sci. Soc. Am. J.*, **62**, 394–400 (1998).
- [3] G. L. Hutchinson and A. R. Mosier, *Soil Sci. Soc. Am. J.*, **45**, 311–316 (1981).
- [4] W. H. Anthony, G. L. Hutchinson and G. P. Livingston, *Soil Sci. Soc. Am. J.*, **59**, 1308–1310 (1995).
- [5] P. Boeckx, O. Van Cleemput and I. Villaralvo, *Soil Biol. Biochem.*, **28**, 1397–1405 (1996).
- [6] A. De Visscher, D. Thomas, P. Boeckx and O. Van Cleemput, *Environ. Sci. Technol.*, **33**, 1854–1859 (1999).
- [7] G. A. F. Seber and C. J. Wild, *Nonlinear regression* (John Wiley & Sons: New York, 1989).
- [8] T. B. Parkin, J. J. Meisinger, S. T. Chester, J. L. Starr and J. A. Robinson, *Soil Sci. Soc. Am. J.*, **52**, 323–329 (1988).